Malaysian Journal of Chemistry, 2023, Vol. 25(3), 295-302
(Special Issue: *3rd IKMPB Online Symposium 2023 - Innovation in Chemistry Towards Sustainable Development*)

The Structural and Morphological Properties of Novel Ag_2CO_3/Nb_2O_5 Composite

Nur Ramadhan Mohamad Azaludin[1], Zul Adlan Mohd Hir[1], Zuraida Khusaimi[2], Nurul Infaza Talalah Ramli[1], Mohd Arif Sarjidan[3], Paweena Dulyaseree[4] and Hartini Ahmad Rafaie[5*]

[1]Faculty of Applied Sciences, Universiti Teknologi MARA Pahang, 26400 Bandar Tun Abdul Razak Jengka Pahang, Malaysia
[2]Centre for Functional Materials and Nanotechnology, Institute of Science, Universiti Teknologi MARA 40450 Shah Alam, Selangor, Malaysia
[3]Low Dimensional Materials Research Center, Department of Physics, Faculty of Science, University of Malaya 50603 Kuala Lumpur, Malaysia
[4]Department of Physics, Faculty of Science Technology and Agriculture, Yala Rajabhat University, 133, Thesaban 3, Sateng, Muang Yala, 95000 Thailand
[5]Centre of Foundation Studies, Universiti Teknologi MARA, Selangor Branch, Dengkil Campus, 43800 Dengkil Selangor, Malaysia
*Corresponding author (e-mail: hartinirafaie@uitm.edu.my)

Ag-based semiconductor materials have recently attracted the attention and research efforts of many material scientists due to its broad range of applications. This study aimed to examine the effect of incorporation of niobium pentoxide (Nb_2O_5) to the structural and morphological properties of silver carbonate (Ag_2CO_3). The synthesis and evaluation on Ag_2CO_3, Nb_2O_5, and Ag_2CO_3/Nb_2O_5 composite were discussed in detailed. Ag_2CO_3, Nb_2O_5, and Ag_2CO_3/Nb_2O_5 composite were synthesized by facile precipitation method at room temperature and were characterized by X-Ray Diffraction (XRD), Fourier Transform Infra-Red (FT-IR) spectroscopy, and Field Emission Electron Microscopy (FESEM) for its structural and morphological properties. XRD patterns revealed that both Ag_2CO_3 and Nb_2O_5 have monoclinic crystal structure. FT-IR analysis showed the existence of CO_3^{2-}, C–O and Nb=O groups, as well as the formation of bridging Nb–O–Nb in the composite matrix. Morphological analysis showed that the Nb_2O_5 particles were irregular spherical- shaped and were well-distributed on the surface of irregular short rod structure of Ag_2CO_3.

Keywords: Structural; morphological; niobium pentoxide; silver carbonate; precipitation

Received: December 2022; Accepted: April 2023

Transition metal oxide semiconductors are a broad class of materials with a variety of applications. These semiconductor-metal nanocomposites provide a novel and practical approach for the synthesis of new materials with targeted optical, electrical, or catalytic capabilities. These materials have a number of possible applications in the fields of optoelectronics, photo-catalysis, plasmonic, and sensing (Aamir, 2021). Recently, substantial amount of interest has been focusing on finding the extensive bandgap of metal oxide semiconductor materials with nanoscale dimensions. Metal oxides are known as the chemical compounds that are formed due to the chemical reactions between cation metals and oxide ions (Srinivasa Varaprasad et al., 2021).

Among many transition metal oxides, silver carbonates (Ag_2CO_3) is a common p-type semiconductor with a moderate band gap of 2.30 eV (539 nm), and a lot of research has also been done on Ag_2CO_3 for its high-performance photocatalytic performance and anti-bacterial properties (Saud et al., 2015). It is also considered to be another significant Ag-based semiconductor materials with a large capacity of absorbing visible light and a relatively narrow bandgap (Arumugam Senthil et al., 2020). However, its use is restricted by its extremely poor stability brought on by photo-corrosion that is due to the creation of metallic Ag (Guo et al., 2015; Saud et al., 2015; P. Wang et al., 2021). Such weakness has prevented its practical application, and several studies have been done to combine Ag_2CO_3 with different materials to improve its properties, stability and application in photocatalysis, such as Ag_2CO_3/ZnO (Sánchez-Cid et al., 2019), (C. Wu, 2014; Xiang et al., 2016), Ag_2CO_3/CeO (C. Wu, 2015), Ag_2CO_3/GO (Chen et al., 2018), Ag_2CO_3/rGO (W. Wang et al., 2017), and Ag_2CO_3/TiO_2 (Feng et al., 2014; L. Wu et al., 2019).

Meanwhile, Nb_2O_5 is an n-type semiconductor with a bandgap energy of 3.0–3.4 eV, and a lot of research has been done on Nb_2O_5 in various fields. Some notable applications of Nb_2O_5 involved the photo-catalytic reduction of waste plastics, the activation of

†Paper presented at the 3rd IKMPB Online Symposium 2023 - Innovation in Chemistry Towards Sustainable Development

hydrocarbons, the photoreduction of CO_2, the selected transformation of amines and alcohols, and also photo-degradation of hazardous organic pollutants (Shao et al., 2015; Su et al., 2021). Furthermore, it has the qualities of not being harmful and long-term stability against chemical and photo-corrosion (de Moraes et al., 2020; Nunes et al., 2020; Shao et al., 2015). These findings point to Nb_2O_5 desirable characteristics and its capability for practical uses (Su et al., 2021). Thus, as reported previously, other Ag-based semiconductor materials, i.e., Ag_3PO_4 has been successfully combined with Nb_2O_5 and yielded an improvement in its properties, stability as well as its application in photocatalysis (Osman et al., 2021; Shao et al., 2015). Therefore, combining another Ag-based semiconductor materials, like Ag_2CO_3 with Nb_2O_5 can be a strong candidate and good opportunity for an enhancement of Ag_2CO_3 characteristics, stability, as well as its application in photocatalysis.

In the present study, the preparation of Ag_2CO_3/Nb_2O_5 composite via a facile chemical precipitation method was investigated as well as the characterization of the prepared samples X-ray diffraction (XRD), field emission scanning electron microscope (FESEM), energy dispersive spectrometer (EDX) and Fourier transform infrared (FT-IR) emphasising on its effect on the structural and morphological properties of the materials. To the best of our knowledge, there are very limited number of studies that proposed the formation of heterojunction between Nb_2O_5 and Ag_2CO_3 in the previous study.

EXPERIMENTAL

Materials

Silver nitrate ($AgNO_3$, ≥ 99%), Sodium carbonate (Na_2CO_3, ≥ 99%) were supplied by R&M Chemicals (Malaysia) and Niobium pentoxide (Nb_2O_5, 99.99%) were supplied by Sigma-Aldrich (Germany). Deionized water was used throughout the experiments. All other reagents were used without further purification.

Preparation of Ag_2CO_3/Nb_2O_5 Composite

The Ag_2CO_3/Nb_2O_5 composite were prepared by facile chemical precipitation method. In this procedure, Nb_2O_5 (0.01 mol) was dispersed into the $AgNO_3$ (0.02 mol) solution prior to sonication for 30 minutes. Next, Na_2CO_3 (0.01 mol) was added to the stock solution with continuous stirring for 1 hour at room temperature. The obtained precipitate was collected and washed with 100 ml deionized water thrice to remove any adsorbed ions on the surface of the precipitate or any other impurities. Following that, the product was dried in an oven at 60°C for 24 hours and the resultant sample was named as Ag:Nb 1:1. For the preparation of pure Ag_2CO_3 similar experimental procedure was employed without additional of Nb_2O_5. The pure Nb_2O_5 was ground before being used throughout the experiments and also used as control sample.

Material Characterisations

The structural properties of pure Ag_2CO_3, Nb_2O_5 and Ag_2CO_3/Nb_2O_5 composite were analysed by X-Ray Diffraction (XRD) on PANalytical X'Pert PRO diffractometer with Cu Kα radiation (λ = 0.154056 nm) at 2θ ranging from 10° to 75°. Fourier transform infrared (FT-IR) spectra were conducted using Perkin Elmer infrared spectrometer using attenuated total reflection (ATR) accessory in the frequency range between 500 to 4000 cm^{-1}. The morphological and elemental composition analysis were characterized by field-emission scanning electron microscope equipped with an electron dispersive X-ray analyser (FESEM-EDX, JEOL JSM-7600F).

RESULTS AND DISCUSSION

X-Ray Diffraction (XRD) Analysis

XRD studies were carried out to investigate the phase structure and crystalline nature of the synthesized samples. Figure 1 portrays the XRD patterns of the prepared pure Ag_2CO_3, Nb_2O_5 and Ag_2CO_3/Nb_2O_5 composite. It was observed that the peaks of diffraction of pure Ag_2CO_3 and Nb_2O_5 were in good agreement with the monoclinic crystal structure of both Ag_2CO_3 (JCPDS No. 01-070-2184) and Nb_2O_5 (JCPDS No. 00-037-1468), respectively. The major diffraction peaks of Ag_2CO_3 are located at 2θ = 18.561°, 20.524°, 28.972°, 32.591°, 33.644°, 37.048°, 39.572°, and 51.359°, which are indexed to (020), (110), (011), (-101), (130), (200), (031), and (150) crystal planes of Ag_2CO_3. The sharp and intense diffraction peaks indicate the good crystalline nature of Ag_2CO_3. The similar crystal structure was also reported by Sánchez-Cid et. al (2019), and Wu. C (2014, 2015) (Sánchez-Cid et al., 2019; C. Wu, 2014, 2015). Meanwhile, major diffraction peaks of Nb_2O_5 are located at 2θ = 23.737°, 24.418°, 25.510°, 31.616°, 32.238°, 38.855°, 47.524°, and 50.987° can be assigned to (110), (-405), (402), (-414), (411), (-713), (704), and (-422) crystal planes of Nb_2O_5. Other researchers also reported the same crystal structure, like Graça and his colleagues (2013) and also Kumari and his partners (2020) (Graça et al., 2013; Kumari et al., 2020). Meanwhile, the XRD patterns of Ag_2CO_3/Nb_2O_5 composite demonstrate that the peaks of diffraction matched to Ag_2CO_3 and Nb_2O_5, which therefore demonstrating that the phase of the composite materials was preserved in its original form (Zul et al., 2018). Furthermore, as seen in the patterns, no shifting of peaks occurred and as the molar ratio of Nb_2O_5 in the composites increased, the intensities of the distinctive peaks of Nb_2O_5 also increased, whilst those of Ag_2CO_3 decreased, and vice versa (Yin et al., 2015).

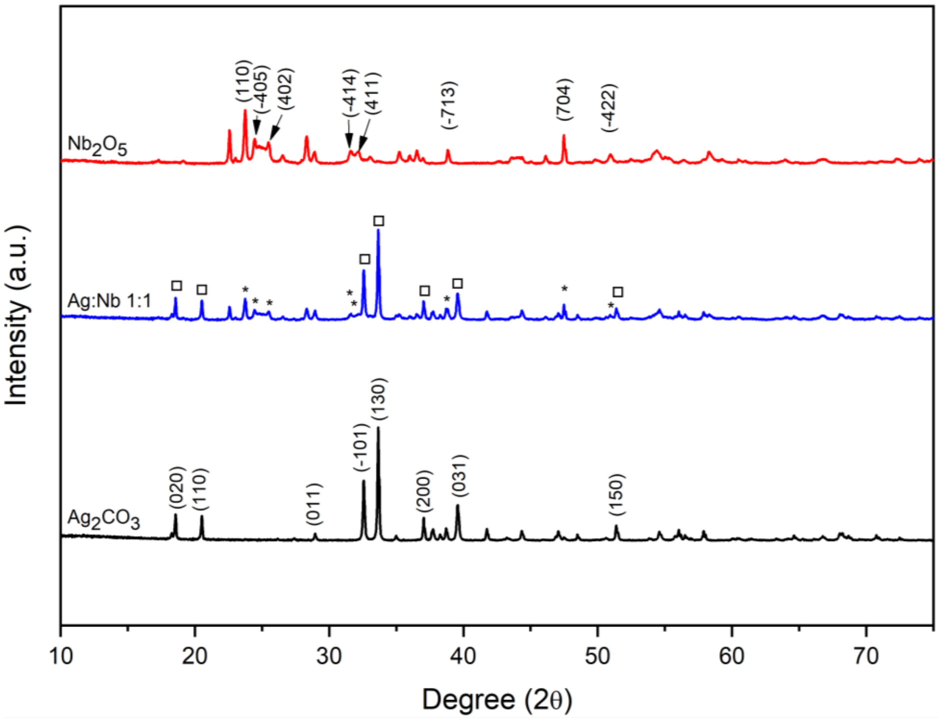

Figure 1. XRD diffraction patterns of the as-prepared Nb_2O_5, Ag_2CO_3 and Ag_2CO_3/Nb_2O_5 (1:1) composite

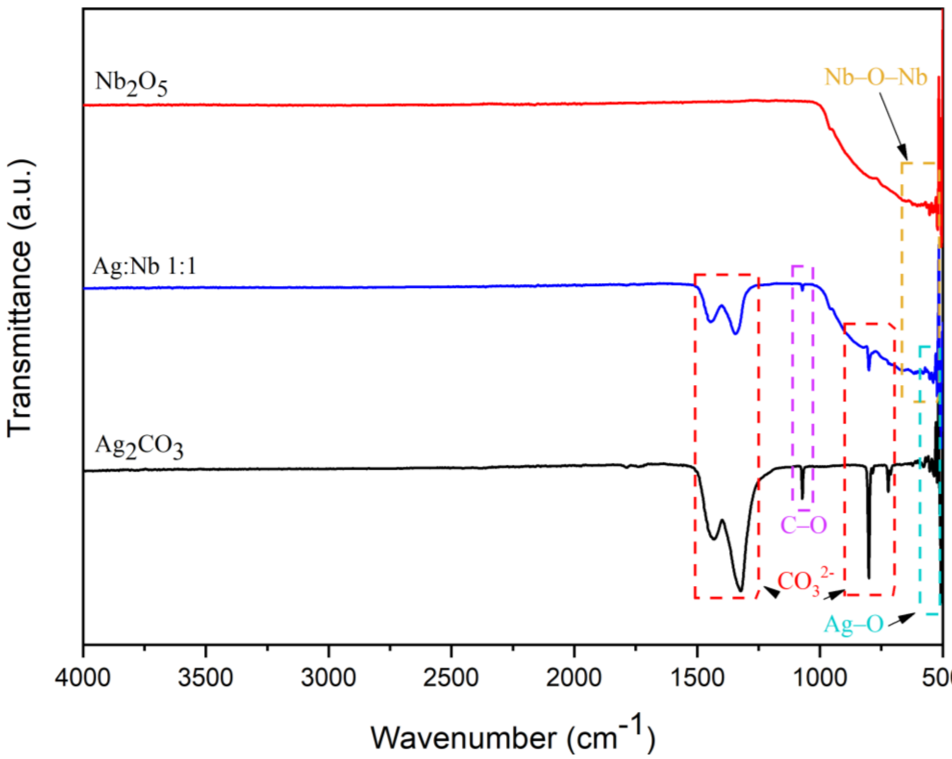

Figure 2. FTIR spectra of the as-prepared Nb_2O_5, Ag_2CO_3 and Ag_2CO_3/Nb_2O_5 (1:1) composite

Fourier Transform Infrared Spectroscopy (FTIR) Analysis

Figure 2 depicts the FT-IR spectra of the prepared pure Ag_2CO_3, Nb_2O_5 and Ag_2CO_3/Nb_2O_5 composite. At wavenumbers around 500 cm^{-1}, the peaks appear to be a Ag–O characteristics for all samples (Rosman et al., 2020). The spectrum of Nb_2O_5 showing at around 500-650 cm^{-1} belongs to the bridging, stretching and angular vibrations of Nb–O–Nb, while a broad shoulder around 948 cm^{-1} is attributed to Nb=O stretching (Peng et al., 2021). In the case of Ag_2CO_3/ Nb_2O_5 spectra, the peaks between 1350-1500 cm^{-1} and around 800 cm^{-1} are attributed to the asymmetric stretching vibration of CO_3^{2-} and symmetric deformation of CO_3^{2-}, respectively (An et al., 2020; Bankole et al., 2022; Liang et al., 2018; Rosman et al., 2020)(Azami et al., 2022; Nyankson et al., 2019; Raizada et al., 2020; Reheman et al., 2019; Rosman et al., 2018; Zhang et al., 2022). Additionally, the CO_3^{2-} bands at the peaks between 1350-1500 cm^{-1}, however, shifted to higher wavenumbers in Ag_2CO_3/ Nb_2O_5 composite. This may be caused by the interactions between Nb–O–Nb and CO_3^{2-} in the Nb_2O_5 and Ag_2CO_3 molecules, respectively (Nyankson et al., 2019; Reheman et al., 2019). Moreover, the peaks at around 1071 cm^{-1} are corresponding to the vibrational stretching of the C–O group (Nyankson et al., 2019).

Surface Morphology and Elemental Composition Analysis

The surface morphology of the prepared pure Ag_2CO_3, Nb_2O_5 and Ag_2CO_3/Nb_2O_5 composite are characterized by FESEM and the results are displayed in Figure 3 (a-c). It can be seen that, the images revealed the formation of pure Ag_2CO_3 is irregular short rod structure while for pure Nb_2O_5, an irregular spherical-shape was displayed in the micrograph (Figure 3a and 3b). The coupling of Ag_2CO_3/Nb_2O_5 composite are observed to have a structure of an irregular spherical-shaped were randomly dispersed on the surface of irregular short rod (Figure 3c). Moreover, substantial agglomeration of the particles was visible in the picture showing the different molar ratios of Ag_2CO_3/Nb_2O_5 composites. Relatively comparable distribution was also reported by Wu and his co-workers (2019) on his Ag_2CO_3@ TiO_2 composite and Zhang et. al (2022) on $ZnFe_2O_4$/ PANI/Ag_2CO_3 (L. Wu et al., 2019) (Zhang et al., 2022).

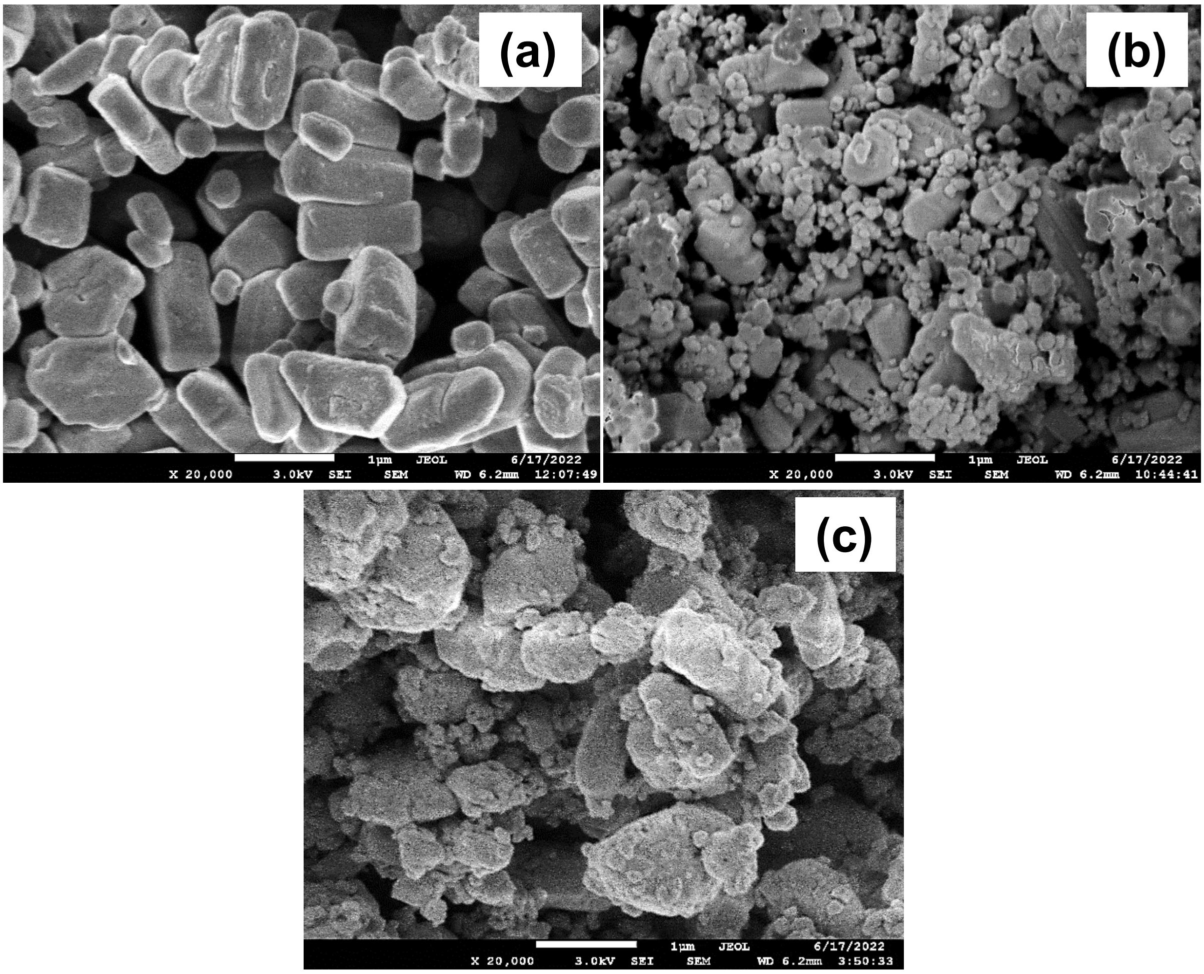

Figure 3. FESEM images of the as-prepared (a) Pure Ag_2CO_3, (b) Pure Nb_2O_5, (c) Ag:Nb 1:1 at 20k magnification

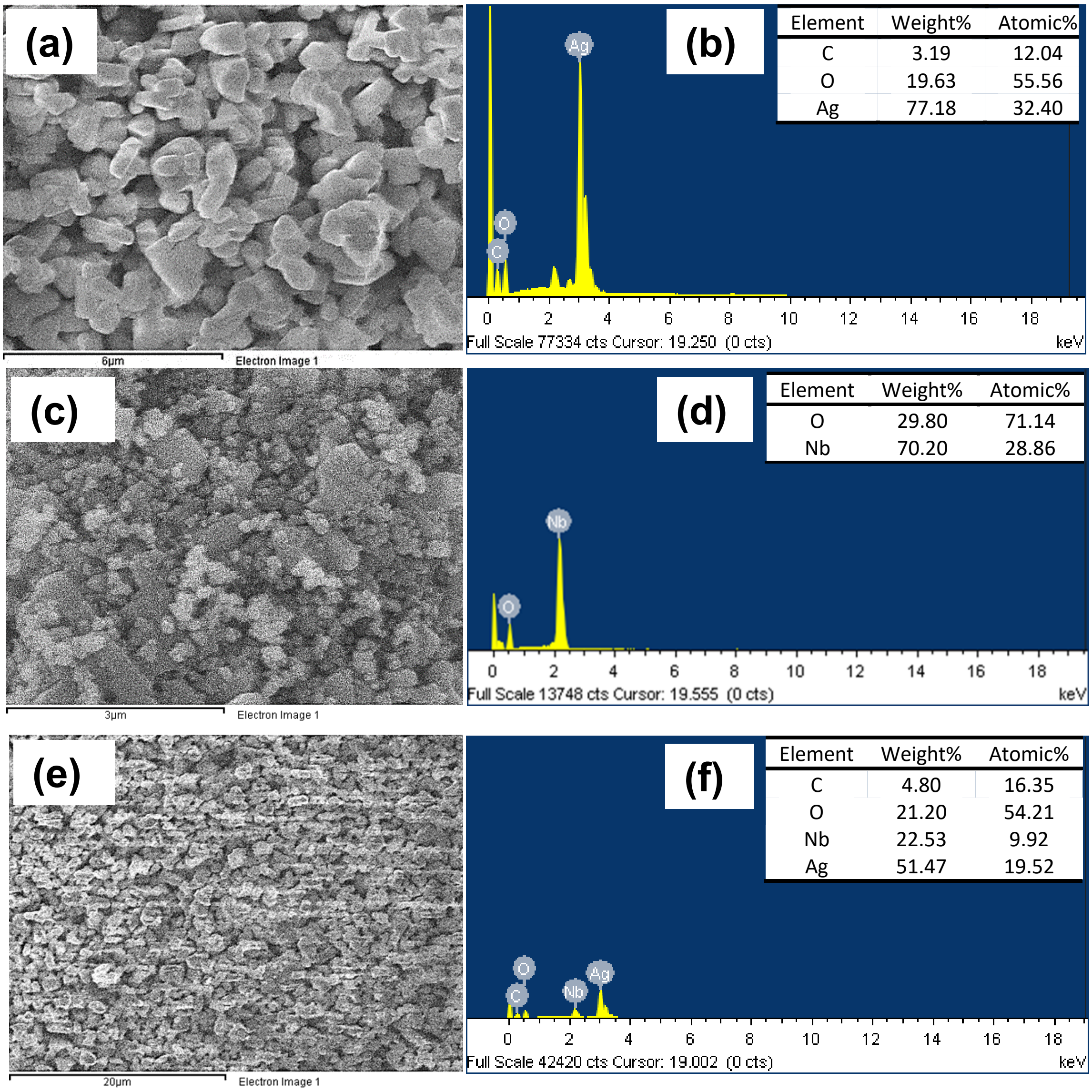

Figure 4. EDX analysis of (a-b) pure Ag_2CO_3, (c-d) pure Nb_2O_5, and (e-f) selected Ag_2CO_3/Nb_2O_5 composite with ratio 1:1

Elemental compositional characterization of pure Ag_2CO_3, Nb_2O_5 and Ag_2CO_3/Nb_2O_5 composite was performed using EDX. In addition, Figure 4 displays the typical EDX spectrum obtained from elemental composition analysis of the prepared pure Ag_2CO_3, pure Nb_2O_5 and selected Ag_2CO_3/Nb_2O_5 composite i.e Ag:Nb 1:1. The EDX analysis reveals the presence of Ag, Nb, C, and O with no additional impurities peak seen, demonstrating the purity of the prepared samples. Moreover, the atomic percent of Ag to Nb element in the EDS analysis is observed to increase in parallel with molar ratios of the materials. The EDX results verified that the prepared samples were composed of Ag_2CO_3 and Nb_2O_5 materials.

CONCLUSION

In conclusion, the Ag_2CO_3/Nb_2O_5 composite were successfully prepared via a simple chemical precipitation method and exhibit irregular spherical-shaped that randomly dispersed on the surface of irregular short rod structure. The XRD patterns revealed that both Ag_2CO_3 and Nb_2O_5 have monoclinic crystal structure with no shifting of peaks occurred. The FT-IR analysis pointed out the existence of several functional groups assigned to their respective stretching vibrations especially for Ag–O (~500cm^{-1}), C–O (1071 cm^{-1}), CO_3^{2-} (~800 cm^{-1} and 1350-1500 cm^{-1}), Nb–O–Nb (500-650 cm^{-1}) and Nb=O (948 cm^{-1}), respectively. Additionally, this study would be a key approach for gaining a thorough grasp of the morphological and structural characteristics on heterojunction coupling system of Ag_2CO_3/Nb_2O_5 composite. The insight knowledge on the properties of the prepared composite could be beneficial for research enhancement and future application such as it can be potentially act as photocatalyst.

ACKNOWLEDGEMENTS

The authors gratefully acknowledge the financial support provided by the Ministry of Higher Education (MOHE) and Universiti Teknologi MARA (UiTM) for the YTR grant (600-RMC/YTR/5/3 (005/2020)), as well as the services and facilities provided to carry out the laboratory work in UiTM Pahang Branch, Jengka Campus and Centre for Functional Materials and Nanotechnology, Institute of Science, UiTM Shah Alam, Selangor.

The authors declare that they have no conflict of interest.

REFERENCES

1. Aamir, L. (2021) Novel p-type Ag-WO_3 nanocomposite for low-cost electronics, photocatalysis, and sensing: synthesis, characterization, and application. *Journal of Alloys and Compounds*, **864**, 158108. https://doi.org/10.1016/j.jallcom.2020.158108.

2. An, W., Sun, K., Hu, J., Cui, W. & Liu, L. (2020) The Z-scheme Ag_2CO_3@g-C_3N_4 core-shell structure for increased photoinduced charge separation and stable photocatalytic degradation. *Applied Surface Science*, **504**. https://doi.org/10.1016/j.apsusc.2019.144345.

3. Arumugam Senthil, R., Khan, A., Pan, J., Osman, S., Yang, V., Kumar, T. R., Sun, Y. & Liu, X. (2020) A facile single-pot synthesis of visible-light-driven AgBr/Ag_2CO_3 composite as efficient photocatalytic material for water purification. *Colloids and Surfaces A: Physicochemical and Engineering Aspects*, **586**. https://doi.org/10.1016/j.colsurfa.2019.124183.

4. Azami, M. S., Jalil, A. A., Aziz, F. F. A., Hassan, N. S., Mamat, C. R., Fauzi, A. A. & Izzudin, N. M. (2022) Exploiting the potential of silver oxo-salts with graphitic carbon nitride / fibrous silica-titania in designing a new dual Z-scheme photocatalyst for photodegradation of 2-chlorophenol. *Separation and Purification Technology*, **292** (April), 120984. https://doi.org/10.1016/j.seppur.2022.120984.

4. Bankole, O. M., Ojubola, K. I., Adanlawo, O. S., Oluwafemi, K. A., Adedapo, A. O., Adeyemo, M. A., Olaseni, S. E., Oladoja, N. A., Olivier, E. J., Ferg, E. E. & Ogunlaja, A. S. (2022) Atmospheric CO_2 mediated formation of Ag_2O-Ag_2CO_3/g-C_3N_4 (p-n/n-n dual heterojunctions) with enhanced photoreduction of hexavalent chromium and nitrophenols. *Journal of Photochemistry and Photobiology A: Chemistry*, **427** (September 2021). https://doi.org/10.1016/j.jphotochem.2022.113800.

5. Chen, H., Xu, H. & Dong, W. (2018) Preparation and Photocatalytic Properties of Ag_2CO_3 / Graphene Composite Photocatalyst. *Journal of Analytical Chromatography and Spectroscopy*, **1(1)**, 1–9. https://doi.org/10.24294/jacs.v1i1.346.

6. de Moraes, N. P., dos Santos, G. S., Neves, G. C., Valim, R. B., da Silva Rocha, R., Landers, R., Caetano Pinto da Silva, M. L. & Rodrigues, L. A. (2020) Development of Nb_2O_5-doped ZnO/Carbon xerogel photocatalyst for the photodegradation of 4-chlorophenol. *Optik*, **219**. https://doi.org/10.1016/j.ijleo.2020.165238.

7. Feng, C., Li, G., Ren, P., Wang, Y., Huang, X. & Li, D. (2014) Effect of photo-corrosion of Ag_2CO_3 on visible light photocatalytic activity of two kinds of Ag_2CO_3/TiO_2 prepared from different precursors. *Applied Catalysis B: Environmental*, 158–159, 224–232. https://doi.org/10.1016/j.apcatb.2014.04.020.

8. Graça, M. P. F., Meireles, A., Nico, C. & Valente, M. A. (2013) Nb_2O_5 nanosize powders prepared by sol-gel-Structure, morphology and dielectric properties. *Journal of Alloys and Compounds*, **553**, 177–182. https://doi.org/10.1016/j.jallcom.2012.11.128.

9. Guo, S., Bao, J., Hu, T., Zhang, L., Yang, L., Peng, J. & Jiang, C. (2015) Controllable synthesis porous Ag_2CO_3 nanorods for efficient photocatalysis. *Nanoscale Research Letters*, **10(1)**. https://doi.org/10.1186/s11671-015-0892-5.

10. Kumari, N., Gaurav, K., Samdarshi, S. K., Bhattacharyya, A. S., Paul, S., Rajbongshi, B. M. & Mohanty, K. (2020) Dependence of photoactivity of niobium pentoxide (Nb_2O_5) on crystalline phase and electrokinetic potential of the hydrocolloid. *Solar Energy Materials and Solar Cells*, **208**. https://doi.org/10.1016/j.solmat.2020.110408.

11. Liang, C., Niu, C. G., Shen, M. C., Yang, S. F. & Zeng, G. M. (2018) Controllable fabrication of a novel heterojunction composite: AgBr and Ag@Ag_2O co-modified Ag_2CO_3 with excellent photocatalytic performance towards refractory pollutant degradation. *New Journal of Chemistry*, **42(5)**, 3270–3281. https://doi.org/10.1039/c7nj04133k.

12. Nunes, B. N., Lopes, O. F., Patrocinio, A. O. T. & Bahnemann, D. W. (2020) Recent advances in niobium-based materials for photocatalytic solar fuel production. In *Catalysts*, **10**, 1. MDPI AG. https://doi.org/10.3390/catal10010126.

13. Nyankson, E., Agyei-Tuffour, B., Annan, E., Yaya, A., Mensah, B., Onwona-Agyeman, B., Amedalor, R., Kwaku-Frimpong, B. & Efavi, J. K. (2019) Ag_2CO_3-halloysite nanotubes composite with enhanced removal efficiency for water soluble dyes. *Heliyon*, **5(6)**. https://doi.org/10.1016/j.heliyon.2019.e01969.

14. Osman, N. S., Sulaiman, S. N., Muhamad, E. N., Mukhair, H., Tan, S. T. & Abdullah, A. H. (2021) Synthesis of an Ag_3PO_4/Nb_2O_5 Photocatalyst for the Degradation of Dye. *Catalysts*, **11(4)**, 458. https://doi.org/10.3390/catal11040458.

15. Peng, C., Xie, X., Xu, W., Zhou, T., Wei, P., Jia, J., Zhang, K., Cao, Y., Wang, H., Peng, F., Yang, R., Yan, X., Pan, H. & Yu, H. (2021) Engineering highly active $Ag/Nb_2O_5@Nb_2CT_x$ (MXene) photocatalysts via steering charge kinetics strategy. *Chemical Engineering Journal*, **421(P1)**, 128766. https://doi.org/10.1016/j.cej.2021.128766.

16. Raizada, P., Sudhaik, A., Singh, P., Shandilya, P., Thakur, P. & Jung, H. (2020) Visible light assisted photodegradation of 2,4-dinitrophenol using Ag_2CO_3 loaded phosphorus and sulphur co-doped graphitic carbon nitride nanosheets in simulated wastewater. *Arabian Journal of Chemistry*, **13(1)**, 3196–3209. https://doi.org/10.1016/ j.arabjc.2018.10.004.

17. Reheman, A., Kadeer, K., Okitsu, K., Halidan, M., Tursun, Y., Dilinuer, T. & Abulikemu, A. (2019) Facile photo-ultrasonic assisted reduction for preparation of rGO/Ag_2CO_3 nanocomposites with enhanced photocatalytic oxidation activity for tetracycline. *Ultrasonics Sonochemistry*, **51**, 166–177. https://doi.org/10.1016/j.ultsonch.2018.10.030.

18. Rosman, N., Salleh, W. N. W., Ismail, A. F., Jaafar, J., Harun, Z., Aziz, F., Mohamed, M. A., Ohtani, B. & Takashima, M. (2018) Photocatalytic degradation of phenol over visible light active $ZnO/Ag_2CO_3/Ag_2O$ nanocomposites heterojunction. *Journal of Photochemistry and Photobiology A: Chemistry*, **364**, 602–612. https://doi.org/10.1016/ j.jphotochem.2018.06.029.

19. Rosman, N., Salleh, W. N. W., Mohamed, M. A., Harun, Z., Ismail, A. F. & Aziz, F. (2020) Constructing a compact heterojunction structure of Ag_2CO_3/Ag_2O in-situ intermediate phase transformation decorated on ZnO with superior photocatalytic degradation of ibuprofen. *Separation and Purification Technology*, **251**. https://doi.org/10.1016/j.seppur.2020.117391.

20. Sánchez-Cid, P., Jaramillo-Páez, C., Navío, J. A., Martín-Gómez, A. N. & Hidalgo, M. C. (2019) Coupling of Ag_2CO_3 to an optimized ZnO photocatalyst: Advantages vs. disadvantages. *Journal of Photochemistry and Photobiology A: Chemistry*, **369**, 119–132. https://doi.org/10.1016/j.jphoto chem. 2018.10.024.

21. Saud, P. S., Pant, B., Ghouri, Z. K., Panthi, G., Park, S. J., Han, W., Park, M. & Kim, H. Y. (2015) Synthesis and characterization of photocatalytic and antibacterial PAN/Ag_2CO_3 composite nanofibers by ion exchange method. *Fibers and Polymers*, **16(6)**, 1336–1342. https://doi.org/10.1007/s12221-015-1336-7.

22. Shao, R., Zeng, X., Cao, Z., Dong, H., Wang, L., Wang, F., Liu, J., Li, Z. & Liang, Q. (2015) A novel Ag_3PO_4/Nb_2O_5 fiber composite with enhanced photocatalytic performance and stability. *RSC Advances*, **5(123)**, 102101–102107. https://doi.org/10.1039/c5ra17555k.

23. Srinivasa Varaprasad, H., Sridevi, P. V. & Satya Anuradha, M. (2021) Optical, morphological, electrical properties of $ZnO-TiO_2-SnO_2/CeO_2$ semiconducting ternary nanocomposite. *Advanced Powder Technology*, **32(5)**, 1472–1480. https://doi.org/10.1016/j.apt.2021.02.042.

24. Su, K., Liu, H., Gao, Z., Fornasiero, P. & Wang, F. (2021) Nb_2O_5-Based Photocatalysts. *Advanced Science*, **8(8)**, 1–25. https://doi.org/10.1002/advs.202003156.

25. Wang, P., Zhao, H., Li, S., Jing, R., Liu, Y., Jiang, N., Bian, F., Liu, Y., Liu, H. & Zhang, Q. (2021) Fabrication of direct Z-scheme black phosphorus nanosheets/Ag_2CO_3 heterojunction photocatalyst with enhanced stability and visible light photocatalytic activity. *Journal of Materials Science*, **56(13)**, 8060–8078. https://doi.org/10.1007/s10853-020-05752-7.

26. Wang, W., Liu, Y., Zhang, H., Qian, Y. & Guo, Z. (2017) Re-investigation on reduced graphene oxide/Ag_2CO_3 composite photocatalyst: An insight into the double-edged sword role of RGO. *Applied Surface Science*, **396**, 102–109. https://doi.org/10.1016/j.apsusc.2016.11.030.

27. Wu, C. (2014) Synthesis of Ag_2CO_3/ZnO nanocomposite with visible light-driven photocatalytic activity. *Materials Letters*, **136**. https://doi.org/10.1016/j.matlet.2014.08.074.

28. Wu, C. (2015) Synthesis of Ag_2CO_3/CeO_2 microcomposite with visible light-driven photocatalytic activity. *Materials Letters*, **152**, 76–78. https://doi.org/10.1016/j.matlet.2015.03.086.

29. Wu, L., Wang, X., Wang, W., Li, J. & Li, X. (2019) Fabrication of amorphous TiO_2 shell layer on Ag_2CO_3 surface with enhanced photocatalytic activity and photostability. *Journal of Alloys and Compounds*, **806**, 603–610. https://doi.org/10.1016/j.jallcom.2019.07.200.

30. Xiang, Z., Zhong, J., Huang, S., Li, J., Chen, J., Wang, T., Li, M. & Wang, P. (2016) Efficient charge separation of Ag_2CO_3/ZnO composites prepared by a facile precipitation approach and its dependence on loading content of Ag2CO3.

Materials Science in Semiconductor Processing, **52**, 62–67. https://doi.org/10.1016/j.mssp.2016.06.001.

31. Yin, L., Wang, Z., Lu, L., Wan, X. & Shi, H. (2015) Universal degradation performance of a high-efficiency $AgBr/Ag_2CO_3$ photocatalyst under visible light and an insight into the reaction mechanism. *New Journal of Chemistry*, **39(6)**, 4891–4900. https://doi.org/10.1039/c5nj00385g.

32. Zhang, R., Zhao, C., Yu, J., Chen, Z. Y., Jiang, J. C., Zeng, K., Cai, L. & Yang, Z. (2022) Synthesis of dual Z-scheme photocatalyst $ZnFe_2O_4$/PANI/Ag_2CO_3 with enhanced visible light photocatalytic activity and degradation of pollutants. *Advanced Powder Technology*, **33(1)**, 103348. https://doi.org/10.1016/j.apt.2021.10.040.

33. Zul, O. N. S., Mohd, A., Hayati, H., Mohd, M., Mastuli, S. & Halim, A. (2018) Designing visible-light-driven photocatalyst of - Ag_3PO_4 / CeO_2 for enhanced photocatalytic activity under low light irradiation. *Journal of Materials Science: Materials in Electronics*. https://doi.org/10.1007/ s10854-018-0306-4.